Applied Mathematical Modelling 34 (2010) 3085–3097

Contents lists available at ScienceDirect

Applied Mathematical Modelling

journal homepage: www.elsevier.com/locate/apm

CFD analysis of pneumatic conveying in a double-tube-socket (DTS®) pipe

Yu Zhang [a,*], Ling Chen [a], Chunxia Zhang [b], Lixin Yu [a], Xiaolin Wei [a], Lvao Ma [b], Chunsheng Guan [b]

[a] Institute of Mechanics, Chinese Academy of Sciences, Beijing 100190, China
[b] China Electric Power Research Institute, Beijing 100055, China

ARTICLE INFO

Article history:
Received 3 June 2009
Received in revised form 21 December 2009
Accepted 29 January 2010
Available online 4 February 2010

Keywords:
CFD
Double-tube-socket (DTS®)
Energy consumption

ABSTRACT

A pipeline with a bypass is widely used for the pneumatic conveying of material. The double-tube-socket (DTS®) technology, which uses a special inner bypass, represents the current state of the art. Here, a new methodology is proposed based on the use of computational fluid dynamics (CFD) to predict the energy consumption of DTS conveying. The predicted results are in good agreement with those from pilot-scale experiments.

1. Introduction

Pneumatic conveying is a method for the transport of powdered and granular materials that meets the requirements of a variety of industrial uses. The conveying system includes a source of compressed carrier gas, a feeding device, a conveying pipeline, and a receiver to separate the conveyed material and the carrier gas. The system is totally enclosed and high, low or negative pressures can be used to convey materials [1]. This form of conveying has become popular in recent years due to its relatively low energy consumption. However, when conveying dense material the pipeline can be blocked due to an overly thick layer of material. Consequently, the use of a bypass is proposed so that air flow in the bypass can hinder the formation of thick layers of material in the main pipe [2]. Since 1980, a bypass has been placed inside main pipelines, and this technology is called the double-tube-socket (DTS®).

The main characteristic of a DTS pipe is that it has a smaller pipe installed at the inside top of the ordinary pipe. There are many nozzles at intervals along the inner pipe. If the DTS pipe becomes blocked by powder, the pressure of the upstream air increases and the airflow is forced into the inner pipe through the last nozzle before the blockage. Air escapes from the next nozzle in the inner pipe faster than the airflow in the main pipe. This nozzle is within the blockage and disturbs the built-up powder, allowing the resumption of the powder flow through the main pipe (Fig. 1).

The DTS pipe reduces the frequency of pipeline blockage, and it is widely used for long-distance conveying of powder. As the national research institute for ash handling technology, the China Electric Power Research Institute (CEPRI) developed its own patented DTS for ash handling. To date, more than 40 DTS ash-conveying systems have been installed in 30 coal-burning power plants in China, where the reliability of DTS has been widely validated by usage.

Until now, the details of the DTS conveying mechanism were not fully understood, and all parameters of the DTS system, such as pressure of the carrier gas, were designed empirically. A huge amount of testing work is needed to make the energy consumption of the system as small as possible.

* Corresponding author. Tel.: +86 10 82544231; fax: +86 10 62561284.
E-mail address: zhangyu@imech.ac.cn (Y. Zhang).

0307-904X/$ - see front matter © 2010 Elsevier Inc. All rights reserved.
doi:10.1016/j.apm.2010.01.014

Nomenclature

g	gas phase
s	particle phase
α	volume fraction
v	velocity
F	body force
R	drag force between phases
P_s	solid pressure
θ_s	solid temperature
$\kappa_{\theta s}$	diffusion coefficient of solid temperature
S_θ	source term of solid temperature
D_θ	dissipation term of solid temperature
e_{ss}	coefficient of restitution for particle collisions
$g_{o,ss}$	radial distribution function

Many difficulties in design for the process industries are related to the behaviors of fluids in turbulent flow, often involving more than one phase. Computational-Fluid-Dynamics (CFD) techniques have great potential to contribute for designing and optimizing these processes [3]. In the past, there have been many research work reported that uses CFD to study two-phase (gas–solid and gas–liquid) flow in pipes [4–6], and in pneumatic conveying [7]. It has been proved that in dilute transport situations realistic CFD predictions of pressure drop, particle holdup, and of choking behavior can be made.

This study has investigated the DTS conveying system by both mathematical modeling and by experiment. The mathematical modeling is built-up based on the finite domain techniques [3]. The governing equations were derived in the form of coupled, non-linear partial differential equations [8]. An Euler–Euler model was used to simulate the system and to predict the movement of both carrier gas and conveyed material. In the experimental work, pressure drop, solid loading rate and gas consumption were monitored online. Furthermore, a simple computational program is proposed that outputs the smallest energy consumption of conveying from the input of only the required solid loading rate and conveying distance. The predicted smallest energy consumption is in good agreement with experiment.

2. Methodology

The whole conveying process can be divided into a developing part and a fully developed part, as shown in Fig. 2. The developing part starts at the outlet of the material storage tank and ends where the flow pattern is first fully developed in the conveying pipeline. The fully developed part is from that location in the pipe to the end of the pipe. It is convenient to study these parts separately but there must be a method to link them together afterwards. The full details of the methodology are presented below.

2.1. Fully developed part

The distance of the material is to be conveyed could be up to a few kilometers. It is expensive in CPU terms to simulate the whole pipeline; however, when the flow achieves the fully developed stage, the flow pattern is periodically changed due to

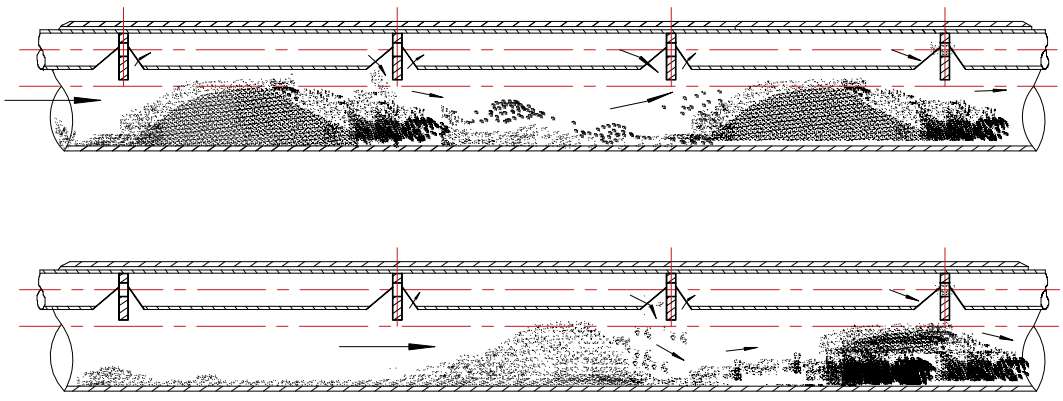

Fig. 1. Principle of double-tube-system conveying pipe.

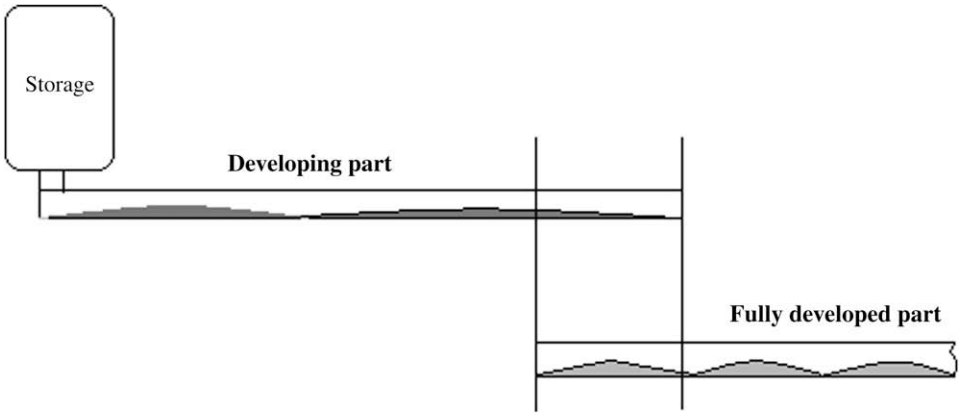

Fig. 2. Developing and fully developed parts.

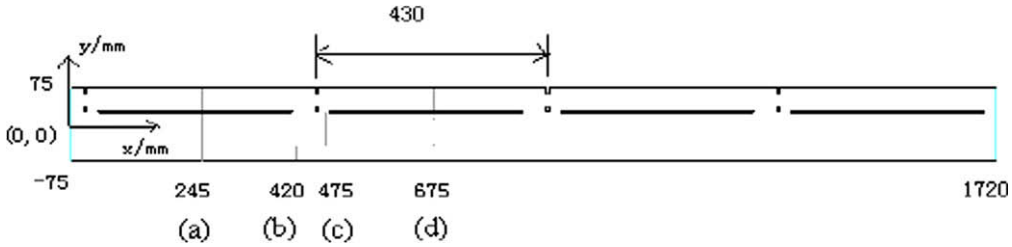

Fig. 3. Sketch of the calculation domain.

the periodic nature of the DTS structure. Therefore, the simulation object is chosen as shown in Fig. 3. There are 4 cross-sections labeled a, b, c, and d in Fig. 3, where the pressure, gas flow-rate and solid loading rate are monitored in the simulation. So that the simulated object can represent the whole of the fully developed part, a periodic boundary condition is used to describe both the inlet and the outlet of the calculation domain. The periodic boundary condition implies that the inlet and the outlet are coupled together. Everything leaving the domain from the outlet will flow into the domain again via the inlet. Consequently, the flow patterns are exactly the same for the inlet and the outlet. The pressure drop from the inlet to the outlet needs to be specified before the computational fluid dynamics (CFD) calculation.

A Euler–Euler model was used to simulate the movements of both carrier gas and conveyed material. The essence of the model is that the particle phase is treated as a continuous phase with its own convection term, diffusion term, source term and dissipation term in its conservation equations. It is well known that all conservation equations for the gas phase are derived from a theory called Molecular Gas Dynamics. It can be supposed that the performance of particles is rather similar to the performance of gas molecules. Hence, all terms of particle conservation equations can be obtained from the Granular Dynamics theory. Full details of the Euler–Euler model are given in references [9,10]. The main concept of a Euler-Euler model is described by the following simplified equations:

$$\frac{\partial}{\partial t}(\alpha_i\rho_i) + \nabla\cdot(\alpha_i\rho_i\vec{v}_i) = 0; \quad i = g,s, \tag{1}$$

$$\frac{\partial}{\partial t}(\alpha_g\rho_g\vec{v}_g) + \nabla\cdot(\alpha_g\rho_g\vec{v}_g\vec{v}_g) = -\alpha_g\nabla P + \nabla\cdot\tau_g + \vec{F}_g + R_{g,s}, \tag{2}$$

$$\frac{\partial}{\partial t}(\alpha_s\rho_s\vec{v}_s) + \nabla\cdot(\alpha_s\rho_s\vec{v}_s\vec{v}_s^{)}) = -\alpha_s\nabla P + \nabla\cdot\tau_s + \vec{F}_s + R_{s,g} - \nabla P_s, \tag{3}$$

$$p_s = \alpha_s\rho_s + 2\rho_s(1+e_{ss})\alpha_s^2 g_{0,ss}\theta_s, \tag{4}$$

$$\frac{\partial}{\partial t}(\alpha_s\rho_s\theta_s) + \nabla\cdot(\alpha_s\rho_s\vec{v}_s\theta_s) = S_\theta + \nabla\cdot(\kappa_{\theta s}\nabla\theta_s) - D_\theta. \tag{5}$$

The most important variables are solid pressure and solid temperature, which represent the random movement of particles. Form Eq. (3), it can be seen, the gas pressure gradient is involved in the particle phase momentum calculation. It has been proved that stable and meaningful results can be obtained with consideration the terms of pressure gradients under the condition that the pressure gradient must be written as the partial gradient of pressure but not the gradient of a partial pressure [11].

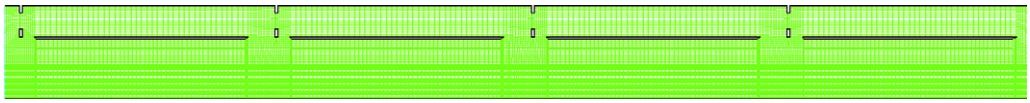

Fig. 4. Arrangement of grids.

2.2. Developing part

The same CFD models are used for prediction of the fluid structure inside the developing part of the DTS system; however, the flow pattern is not periodically changed in that part. The velocity profiles for both phases need to be specified at the inlet

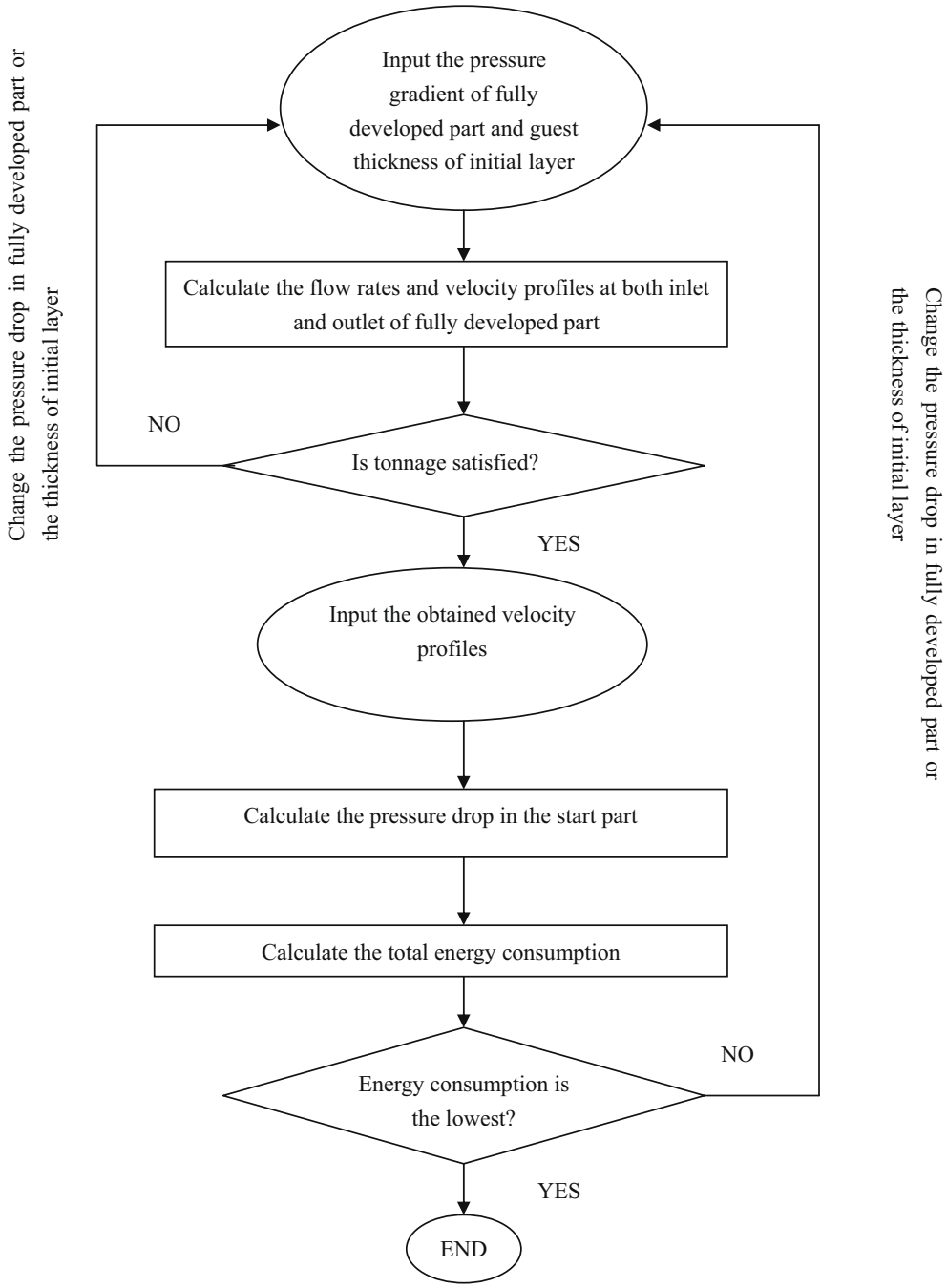

Fig. 5. The methodology.

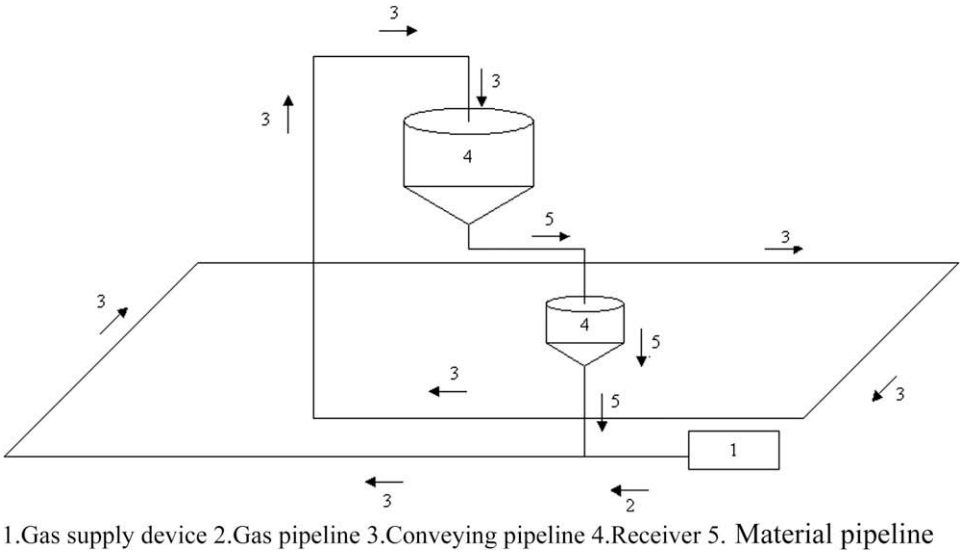

Fig. 6. The sketch of the experimental system.

and at the outlet of the calculation domain. Furthermore, because of mass balance and the conservation of momentum, the velocity profiles at the outlet of the developing part must be the same as those at the inlet of the fully developed part.

2.3. Computational details

The 2D arrangement of 15579 grids is shown in Fig. 4. The grids are not uniform but are arranged on the basis of structure. The largest grid area is 8.985996 e-3 m^2 while the smallest is 1.258492 e-3 m^2. In order to make the periodic boundary conditions effective, the calculation domain must contain at least 4 interval nozzles, as shown in Fig. 4. The relaxation factors for solving conservation equations can be set as 0.5–0.8, it depends on cases. The calculation is unsteady and the time step could not be greater than 0.001 s for getting stable solutions. Therefore, although the simulation object is only 1.7 m long, in average, running one case until convergence takes 21 days using a computer with core 2 2.0 GHz CPU.

2.4. Coupling method

Fig. 5 illustrates the methodology that can couple both parts together.

1. Using the pressure gradient of the fully developed part to calculate the velocity profiles inside that part.
2. Applying the obtained velocity profiles as the outlet boundary conditions of the developing part to calculate the pressure drop in that part.

Table 1
Physical properties of conveyed material.

Real density (kg/m^3)	Mean density (kg/m^3)	Deposit angle (°)	Internal friction angle (°)	Diameter (μm)
2120	793.15	40	41	14.28

Table 2
Experimental results.

Test number	Dp (Kpa/m)	Tonnage (t/h)	Ratio between tonnage and gas consumption (kg/kg)	Energy consumption for unit tonnage (kw .h/t .m)
1	0.77	8.44	37.10	0.004817
2	0.92	4.32	29.42	0.007159
3	0.86	6.54	30.58	0.006476
4	0.78	7.21	28.47	0.006314
5	0.72	8.51	30.61	0.005436
6	0.66	8.96	25.63	0.005932
7	0.54	8.38	20.10	0.006240
Average	0.75	7.48	28.85	0.006959

3. Calculate the total energy consumption.
4. Repeat steps 1–3 to do parametric studies.
5. Investigate energy consumption on the basis of all the results.

3. Experimental work

The experimental system consists of four parts. They are the compressed gas supply device, the feeding device, the conveying pipeline and the receiver to separate the conveyed material from the carrier gas. The detailed arrangement of the four parts is shown in Fig. 6. Pressure detectors are set up along the pipeline so that the pressure change can be monitored at different positions. Furthermore, there are mass meters at the outlet of the feeding device, and the variations of solid loading rate are recorded at set time intervals [12,13]. The physical properties of the conveyed material are summarized in Table 1. The conveyed material is coal ash, which is always conveyed at low velocity but in high bulk density [14]. The measured pressure drop, the mass ratio between the conveyed material and the carrier gas, and the energy consumption per unit solid loading rate are given in Table 2. It should be pointed out that in reality those parameters change at different times. Therefore, the time-averaged experimental results are used for comparison with the CFD simulation results. It has been proved experimentally that the unit energy consumption given in Table 2 is the lowest for conveying ash 500 m at 7.48 t/h.

4. Results and discussion

The contours of volume fractions of conveyed material at different times are shown in Fig. 7. At the beginning, piles of material are formed due to the impact of the air jet from the nozzles of the bypass. Once these piles are formed, they keep moving in the direction of the pressure drop. At the beginning, the heights of piles at different locations are almost the same; however, as time passes, the heights of piles are minimized until they are stable. This tendency implies that the structure of the DTS system naturally reduces the height of the piles of material and, therefore, it can minimize the frequency of pipeline blockage.

Fig. 8 shows the volume fraction of conveyed material at the same location at different times. There must be a layer of material formed on the bottom of the pipeline before conveying is stable; however, the initial thickness of that material layer is unknown in a real test. In Fig. 8, the initial thickness of the layer of material is assumed to be 0.03 m for case A, and 0.06 m for case B. It can be seen from Fig. 8(a) and 8(b) that the volume fractions change periodically. When the pile peak reaches the monitoring point, the recorded volume fraction will be the highest, whereas the recorded volume fraction will be the

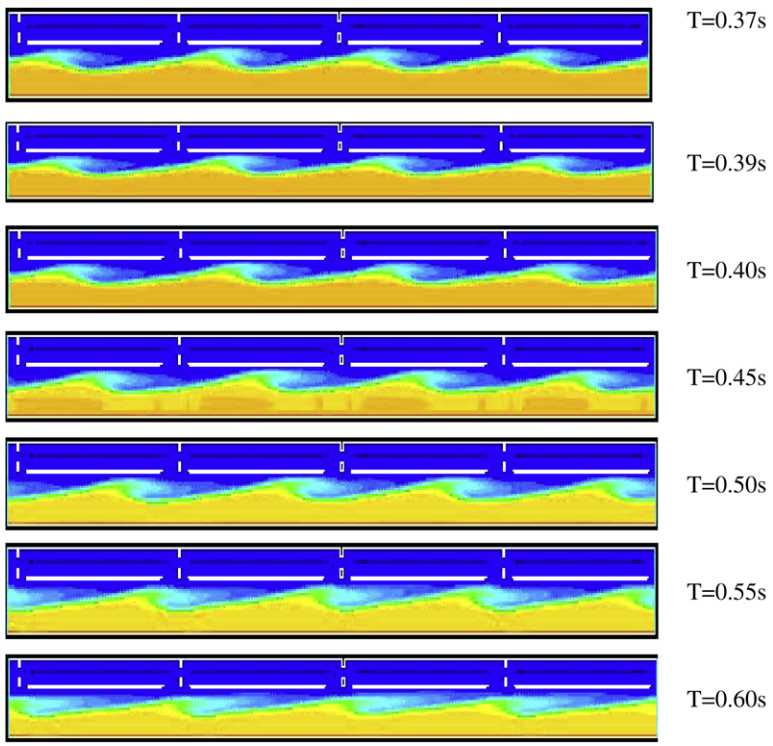

Fig. 7. The contours of volume fraction of conveyed material at different moments.

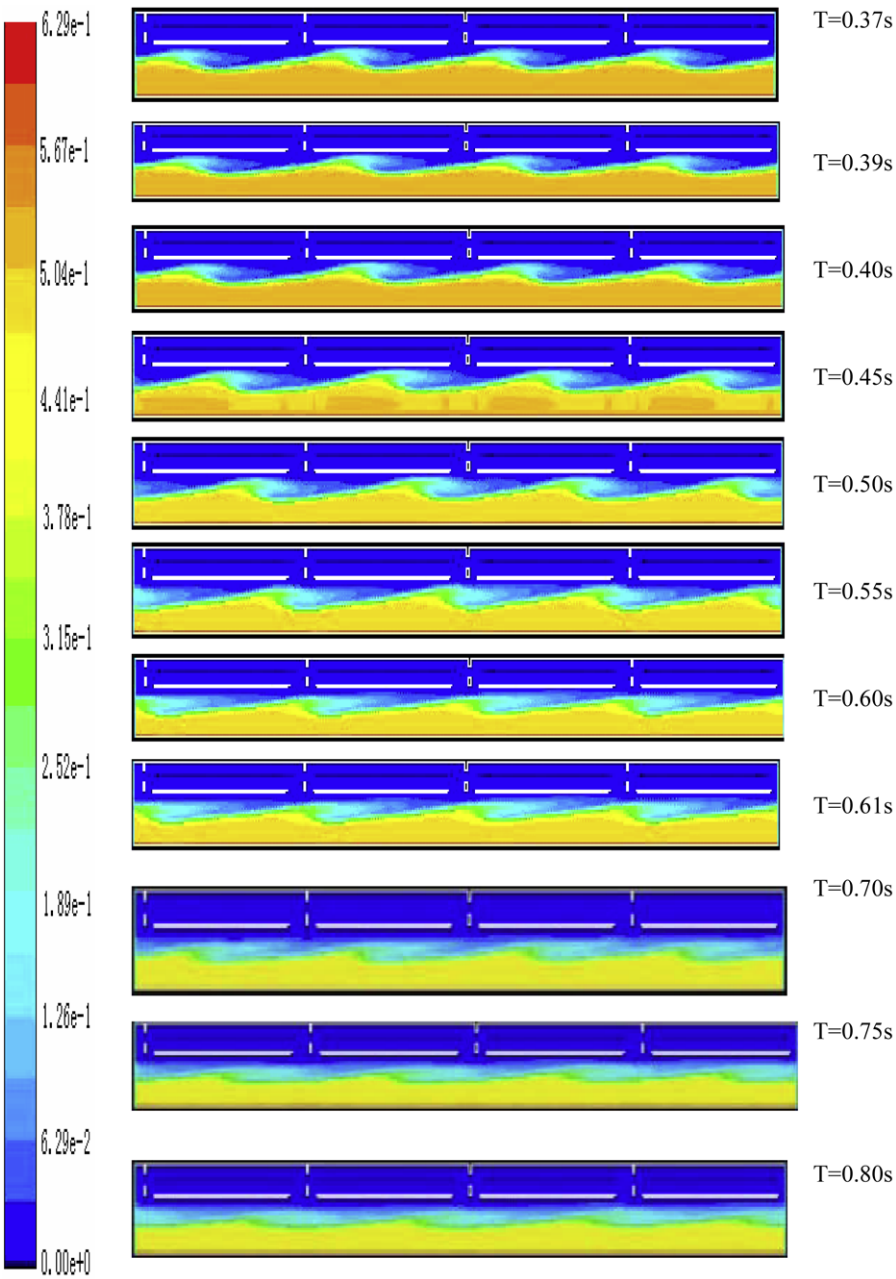

Fig. 7 (*continued*)

lowest when the lowest pile arrives. Therefore, the periodic change of volume fraction at a certain position is the same as the period of the material pile movement. It can be seen that the histories of volume fraction at positions a and d are exactly the same, because the distance between a and d is equal to the distance between the nozzles in the bypass. A comparison of Fig. 8(a) and 8(b) shows that the volume fraction in Fig. 8(a) is much lower than that in Fig. 8(b). This is because the initial layer of material is much thinner for case A.

The velocity of material at the outlet is shown in Fig. 9. For case A, the initial thickness of the layer of material is 0.03 m. The carrier gas passes mainly through the main pipe; consequently, the gas velocity is highest at the center of this pipe. The material is pushed by the gas and the highest velocity of conveyed material occurs at the center of the ordinary pipe. For case B, the initial thickness of the layer of material is 0.06 m. There is less room in the main pipe for the gas to pass through and so most of the gas flows through the bypass.

Fig. 10 shows the volume fractions of material conveyed along the main pipe. It can be supposed that the volume fraction of the highest pile of material is defined as 0.3. Then the height of the pile of material can be identified. The piles of material

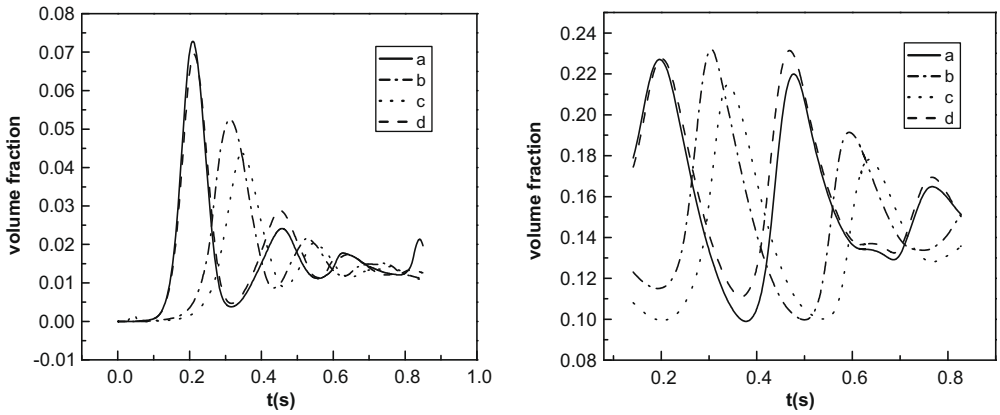

(a) h=30mm (b) h=60mm

Fig. 8. The volume fraction of conveyed material at the same location for different moments.

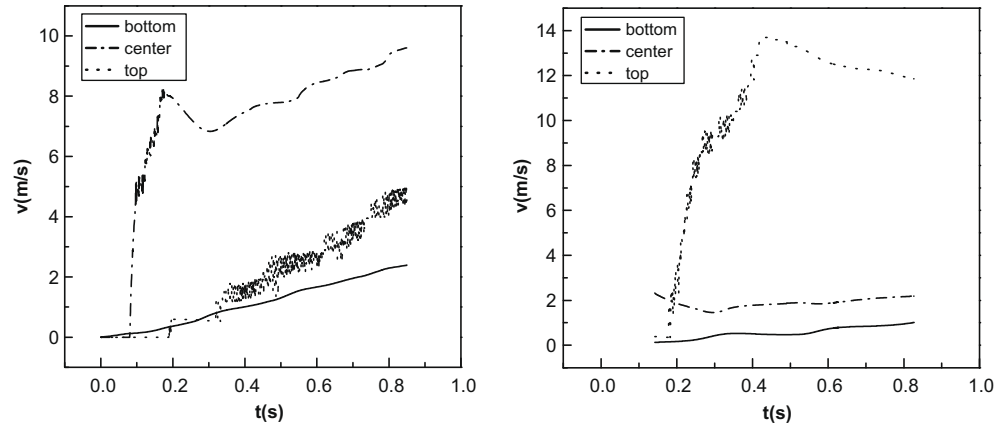

(a) h=30mm (b) h=60mm

Fig. 9. The velocities of conveyed material at different location .

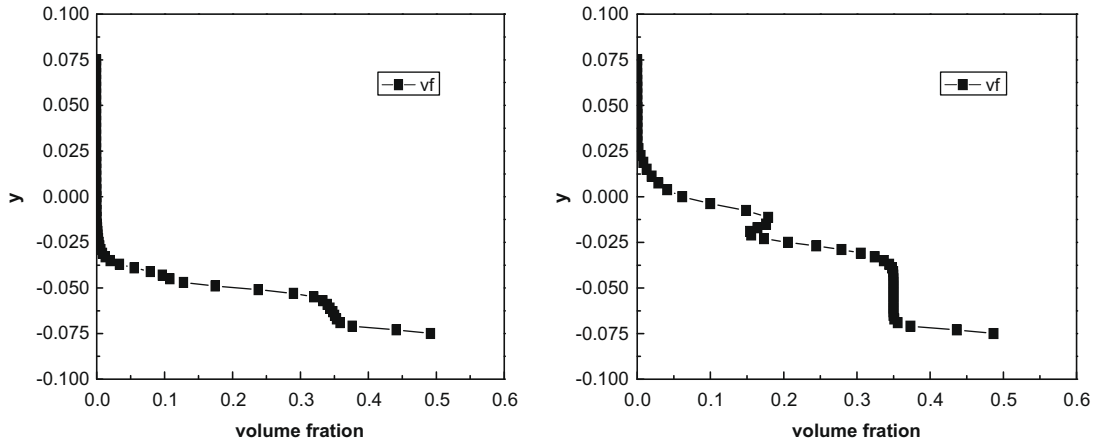

(a) h=30mm (b) h=60mm

Fig. 10. The volume fraction of conveyed material at different locations.

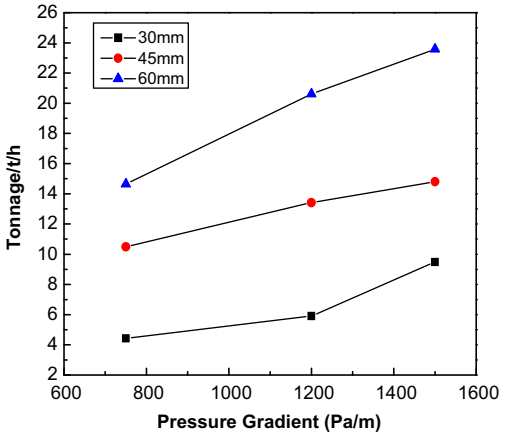

(a) Tonnages under different pressure drops.

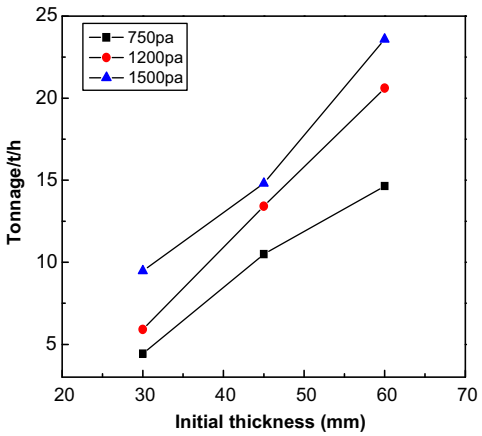

(b) Tonnages under different thicknesses of initial layer

Fig. 11. Tonnage under different conditions.

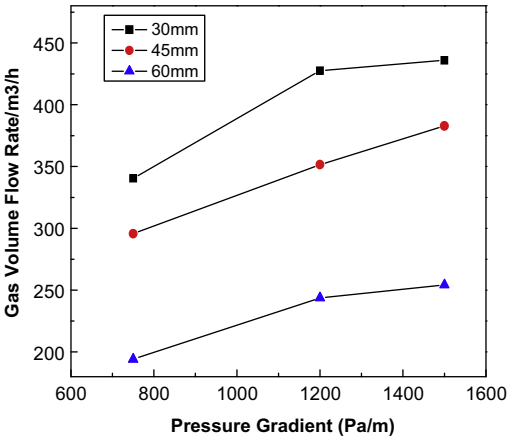

(a) Gas consumption under different pressure drops.

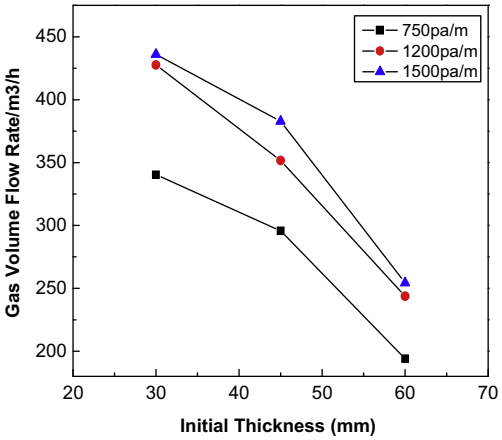

(b) Gas consumption under different thicknesses of initial layer

Fig. 12. Gas consumption under different conditions.

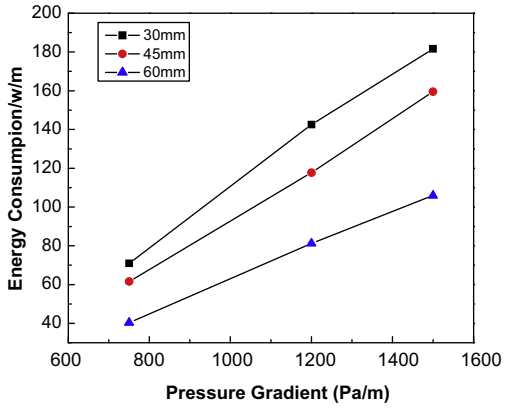

(a) Energy consumption under different pressure drops

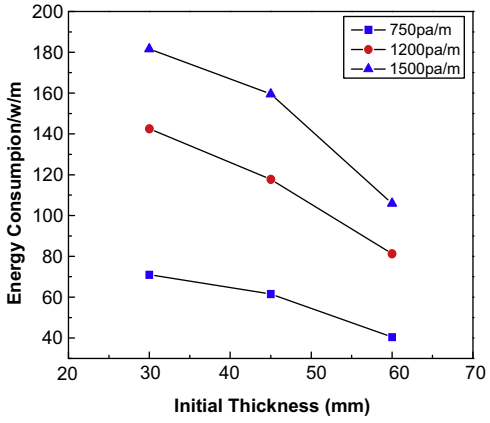

(b) Energy consumption under different thicknesses of initial layer

Fig. 13. Energy consumption.

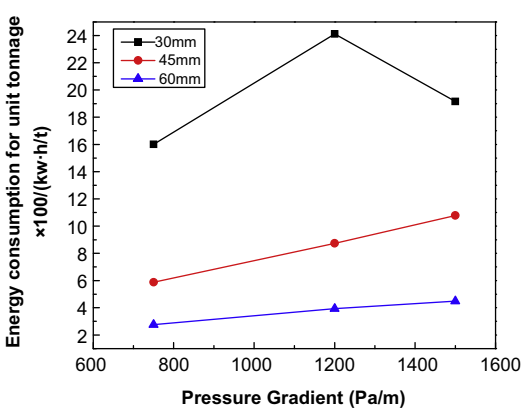

(a) Energy consumptions under different pressure drops

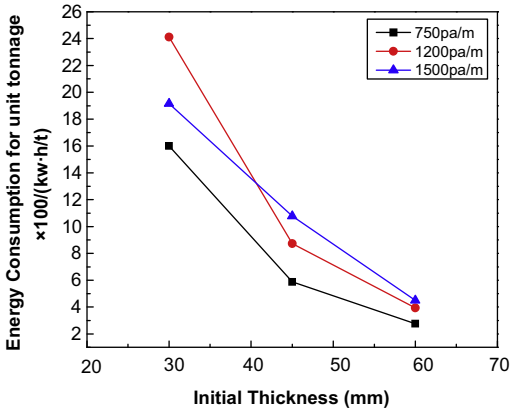

(b) Energy consumptions under different initial thicknesses of initial layer

Fig. 14. Energy consumption for unit tonnage.

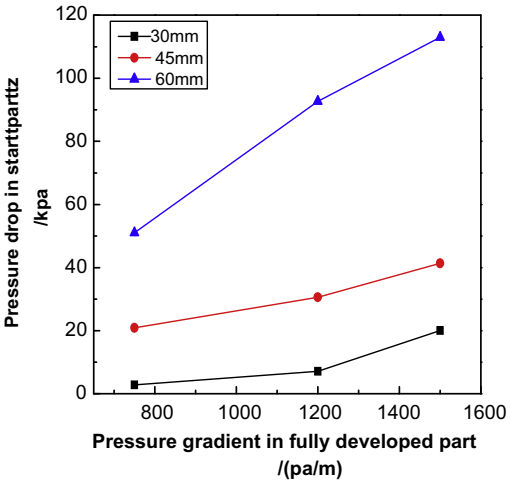

(a) Pressure drops in developing part under different pressure

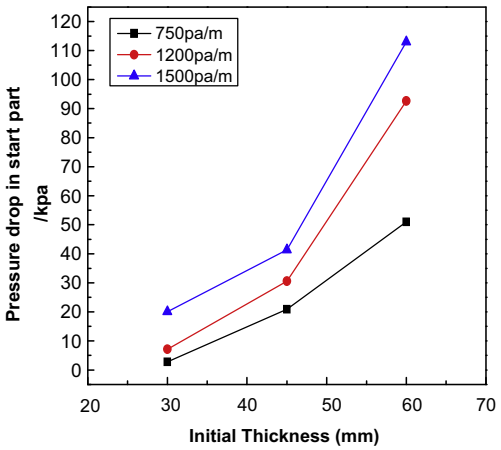

(b) Pressure drops in developing part under different initial thicknesses of initial layer

Fig. 15. The pressure drop in developing part.

are 0.04 m high for case A and 0.07 m high for case B. Therefore, it can be concluded that although the initial thicknesses of the layers of material are different, the increase of the height of the pile is the same (0.01 m) under the same pressure drop (750 Pa/m).

Fig. 11 shows the solid loading rates under different conditions. Fig. 11(a) gives the solid loading rates at different pressure drops, and it can be seen that the solid loading rate increases as the pressure drop increases. Fig. 11(b) shows the solid loading rates at different thicknesses of the initial material layer, and it can be seen that the thickness of the initial layer increases, the solid loading rate increases.

Fig. 12 shows the gas consumption under different conditions. Fig. 12(a) demonstrates that the gas consumption increases as the pressure drop increases, because more gas flows through the main pipe. Fig. 12(b) shows gas consumption with different thicknesses of the initial layer of material. It can be seen that gas consumption decreases with increased thickness of the layer of material because there is less room for the gas to pass through.

Energy consumption is shown in Fig. 13. Energy consumption increases as the pressure drop increases, as shown in Fig. 13(a). From Fig. 13(b) it can be seen that energy consumption decreases as the thickness of the initial layer of material increases. It should be pointed out that although a thicker layer of material helps to save energy in the fully developed part, if the material layer is overly thick the particles will flow into the bypass and thereby the pipeline will be blocked.

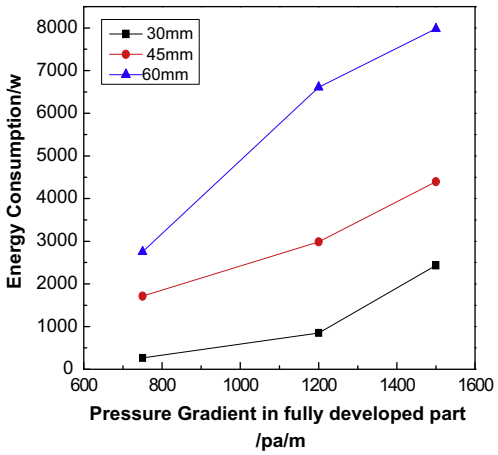

(a) Energy consumptions under different pressure drops in fully developed part

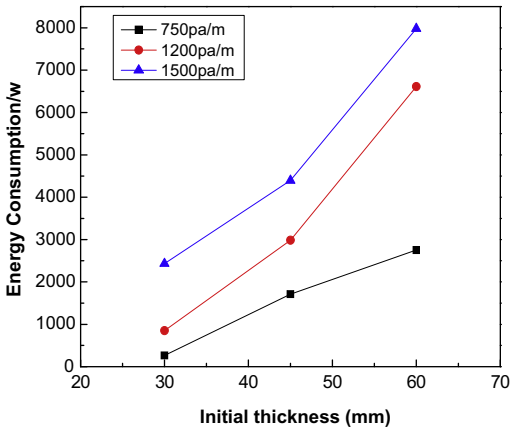

(b) Energy consumptions under different initial thicknesses of material layer

Fig. 16. The energy consumption in developing part.

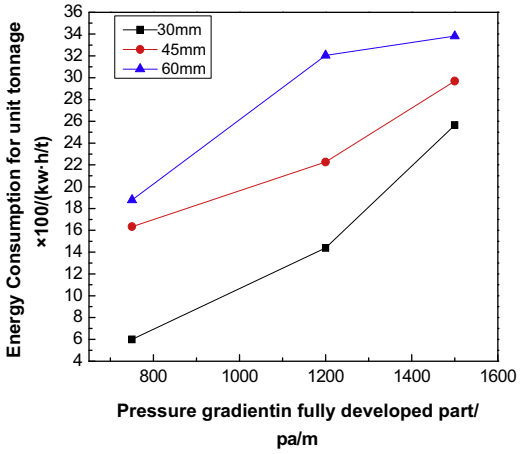

(a) Energy consumptions for unit tonnage under different pressure drops in fully developed part

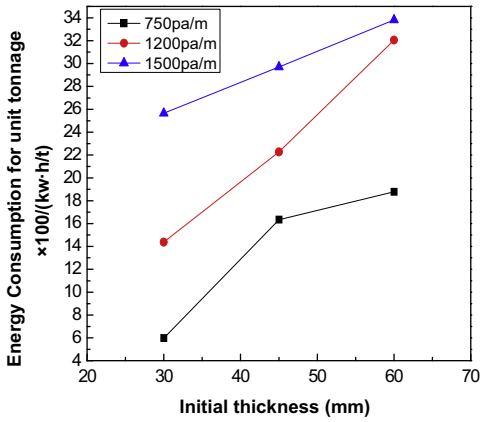

(b) Energy consumptions for unit tonnage under different initial thicknesses of initial layer

Fig. 17. The energy consumption for unit tonnage in developing part.

Fig. 14 shows the energy consumption per unit solid loading rate, which is a very important parameter for evaluation of the efficiency of a conveying system. Fig. 15(a) shows that, in general, the energy consumption per unit solid loading rate increases as the pressure drop increases. However, when the initial thickness is 30 mm, the energy consumption per unit solid loading rate first increases and then decreases. The highest energy consumption point occurs when the pressure drop reaches 1200 Pa/m. Fig. 14(b) shows that as the thickness of the initial layer increases, the energy consumption per unit solid loading rate decreases.

The length of the developing part was chosen as 4.2 m to keep the outlet in the fully developed stage. The pressure drops in the developing part are shown in Fig. 15. It can be seen from Fig. 15(a) that as the pressure drop increases in the fully developed part, the pressure drop in the developing part increases also. Fig. 15(b) shows that as the thickness of the initial layer increases, the pressure drop increases greatly in the developing part.

Energy consumption in the developing part increases as the pressure drop increases in the fully developed part (Fig. 16(a)) and as the thickness of the initial layer of material increases (Fig. 16(b)). A thicker layer of material helps to save energy in the fully developed part but it induces high energy consumption in the developing part.

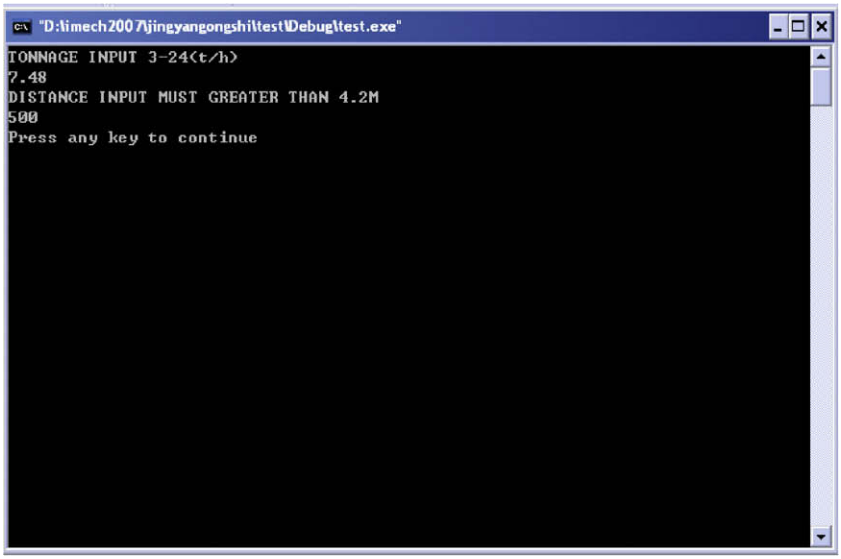

(a) input

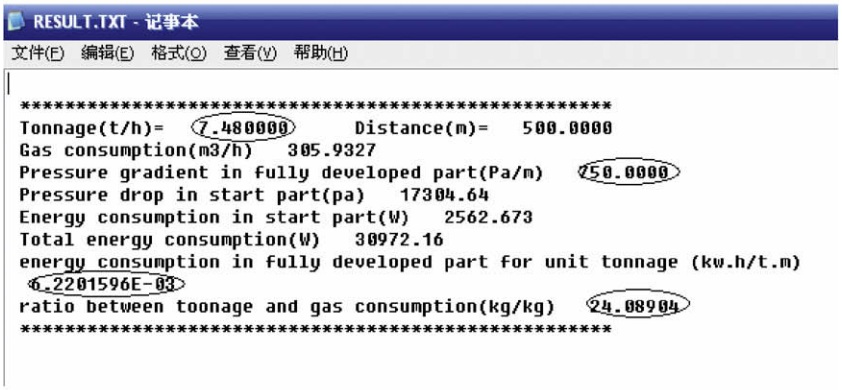

(b) Output

Fig. 18. The calculated best parameters for lowest energy consumption.

Table 3
Comparison and validation.

	Pressure gradient in fully developed part (Pa/m)	Ratio between tonnage and gas consumption	Energy consumption for unit tonnage in fully developed part (kw.h/t.m)
Experimental results	750	28.850	0.006959
Calculated results	750	24.089	0.006220
Error (%)	0.0	16.5	10.6

Energy consumption per unit solid loading rate increases as the pressure drop in the fully developed part increases (Fig. 17 (a)), and as the thickness of the initial layer of material increases (Fig. 17(b)).

A mathematical interpolation method was established and a computational program was devised on the basis of the results discussed above. If solid loading rate and conveying distance are used as input, the computational program will give the optimized air dynamic parameters so that the conveying system will have the lowest energy consumption possible. Fig. 18 (a) shows an input solid loading rate of 7.4 t/h and a conveying distance of 500 m, which match the experimental parameters. The output result in Fig. 18(b) shows that for conveying this solid loading rate for 500 m, the pressure drop in the fully developed part should be 750 Pa/m, the ratio between solid loading rate and gas consumption should be 24.089, and the lowest energy consumption per unit solid loading rate should be 6.22 e-3 kw .h/t. m. Table 3 shows that the experimental results and the calculated results are very similar with an error of <20%, which is acceptable for industrial usage.

5. Conclusion

- A new methodology based on CFD simulation is proposed. This method can be used to study the fluid structures inside the developing and the fully developed parts of DTS separately, and can then couple them together.
- The solid loading rate and energy consumption increase as the pressure drop in the fully developed part increases, which is not desirable.
- The solid loading rate increases and the energy consumption per unit solid loading rate decreases in the fully developed part as the thickness of the initial layer of material increases; however, the energy consumption per unit solid loading rate increases in the developing part. Therefore, simply increasing the thickness of the initial layer of material is not satisfactory.
- Finally, a mathematical method is established for optimization of the parameters of the carrier gas to meet the requirement of solid loading rate and conveying distance with the lowest energy consumption. This method is validated by experiment.

Acknowledgment

This work is supported by the CAS Innovation Program.

References

[1] David Mills, Pneumatic Conveying Design Guide, second ed., Elsevier, 2004.
[2] Huang Biao, Pneumatic Conveying, Shanghai Science and Technology Publisher, 1984.
[3] N.C. Markatos, Mathematical modeling of single and two-phase flow problems in the process industries, Rev. l'Institute Francais du Petrole 48 (6) (1993) 631–662.
[4] K.N. Theologos, N.C. Markatos, Modeling of flow and heat transfer in fluidized catalytic cracking riser-type reactors, Chem. Eng. Res. Des. 70 (A3) (1992) 239–245.
[5] E.D. Koronaki et al, Numerical study of turbulent diesel flow in a pipe with sudden expansion, Appl. Math. Model. 25 (4) (2001) 319–333.
[6] N.C. Markatos, A.K. Singhal, Numerical analysis of one-dimensional, two-phase flow in a vertical cylindrical passage, Adv. Eng. Softw. (1978) 4 (3) (1982) 99–106.
[7] K.N. Theologos, N.C. Markatos, Modeling of vertical pneumatic conveying hydrodynamics, Appl. Math. Modell. 18 (6) (1994) 306–320.
[8] N.C. Markatos, Computational fluid flow capabilities and software, Ironmaking Steelmaking 16 (4) (1989) 266–273.
[9] D Gidaspow, Multiphase Flow and Fluidization–Continuum and Kinetic Theory Description, Academic Press, Boston, 1994.
[10] Fluent 6.3 User Guide.
[11] N.C. Markatos, Modeling of two-phase transient flow and combustion of granular propellants, Int. J. Multiphase Flow 12 (6) (1986) 913–933.
[12] Test report of DTS ash handing system, Electric Power Construction Research Institute, 2001.
[13] Li Xiangyang, Study of the mechanism of gas–solids two-phase flow inside double-tube-socket (DTS®) Pipe, in: International Symposium on Pneumatic Conveying Technologies, 2007, pp. 200–206.
[14] G. Pavoni, Fluidstat: Low velocity conveying of coal-fired boiler fly ash, in: The Third Israeli Conference for Conveying and handling of Particle Solids, Dead Sea, Israel, May, 2000, pp. 10.130–10.136.